

# Energy Absorption Characteristics of Thin-walled Steel Tube Filled with Paper Scraps

Peng Cheng,<sup>a</sup> Qingchun Wang,<sup>a,\*</sup> and Shi Ke<sup>b</sup>

The specific energy absorption of a thin-walled tube can be improved by filler. This study examined the potential use of a cheaper biomass filler, paper scraps, to enhance the energy absorption characteristics of the structure while reducing its cost, compared to that with a traditional filler such as foam material. Quasi-static crushing tests and finite element simulations were performed by using the explicit non-linear finite element software LS-DYNA to determine the improvements to the mean crushing force and specific energy absorption of the steel tube when filled with different densities of paper scraps. The mean crushing force and specific energy absorption of the empty tube, the paper scraps, and thin-walled tube filled with paper scraps were determined, and corresponding numerical simulations were performed. The simulation and test results showed that the impact performance of tube filled with paper scraps was greatly improved when paper scraps density was 0.35 g/cm<sup>3</sup>. By optimizing paper scraps filling structure, a new structure that could further enhance the specific energy absorption was obtained. The optimal scheme could increase the specific energy absorption of Q345 steel tube by 11.35%.

*Keywords:* Biomass; Paper scraps; Specific energy absorption; Numerical simulation; Quasi-static crushing test

*Contact information:* a: School of Technology, Beijing Forestry University, No. 35 Qinghua East Road, Haidian District, Beijing 100083, China; b: Qingdao Automotive Research Institute of Jilin University, No. 1 Loushan Road, Licang District, Qingdao, Shandong 266041, China;

\* Corresponding author: wangqingchun@bjfu.edu.cn

## INTRODUCTION

In recent years, with the rapid increase of car ownership, more traffic accidents have occurred, causing many casualties and great economic losses (Xiong 2018). Therefore, it is of great social and economic importance to improve the crashworthiness of automobile structures. Meanwhile, safety, energy savings, and environmental protection have become the three major themes of automobile development (Wang 2016). These themes focus attention on fuel economy, the manufacturing costs of energy absorption structures, and exhaust emissions when improving vehicle collision safety, instead of simply relying on traditional methods, such as increasing the thickness of the energy absorption structure, to improve crash safety. Consequently, a good way to improve the energy absorption performance of thin-walled tube is by filling it with foam-like materials (Tang 2018; Yang *et al.* 2019).

Thin-walled metal tube is a common energy absorber and is widely used in the automobile, ship, and aerospace industries, among others (Baroutaji *et al.* 2017). Advantages of foam-like materials include low density and high impact energy absorption capacity. They can produce large deformations on certain stress platforms when

compressed, which can help buffer the effects of energy absorption (Goel 2015). Therefore, filling thin-walled metal tubes with foam-like materials has become an active research subject in this area.

Foam aluminum is a typical filler for thin-walled metal tubes. The effects of aluminum foam filling on the energy absorption of thin-walled tubes have been studied by many scholars. Hanssen *et al.* (1999, 2000) performed axial impact tests on thin-walled square and circular tubes filled with aluminum foam and obtained empirical formulas for mean crushing force of two structures under axial crushing. Chen and Wierzbicki (2001) analyzed and numerically studied the axial crushing of empty multi-cell columns, derived a theoretical solution of the mean crushing force of the multi-cell cross-section, and proposed that the interaction between the foam core and the column wall can significantly enhance the energy absorption effect of the structure. Wang *et al.* (2004, 2005) conducted quasi-static axial crushing tests on aluminum foam-filled hat sections that were made of steel, showing that the mean crushing force and specific energy absorption of the structure were higher than those of the unfilled structure, and greater aluminum foam density resulted in greater improvement. Gao and Xu (2016) studied the dynamic impact properties of aluminum-foam-filled parts, showing that the initial peak value of impact acceleration is mainly determined by the thickness of the aluminum shell, and the impact isolation efficiency decreases with increasing shell thickness. Ying *et al.* (2018) conducted an impact test on the energy absorbing specimen filled with aluminum foam and found that the plastic deformation of the steel plate and the compaction of the aluminum foam achieve the absorption and consumption of impact energy.

Aluminum foam is a good energy-absorbing filler material for thin-walled metal tubes. However, the preparation process of foamed aluminum is complicated and expensive (Jing *et al.* 2012; Zhang and Ou Yang 2020). Therefore, finding a new filler material that can replace foam aluminum is of great significance to popularize the filling method to improve the energy absorption characteristics of thin-walled tubes.

In research on the crushing and energy absorption of biomass materials, Ali *et al.* (2010) proposed using a biomass material extracted from banana peels as a filler, showing that, compared with the unfilled composite hierarchical structure, the biomass-filled composite hierarchical structure exhibited excellent energy absorption performance at the expense of higher reaction load. The biomass crushing molding process is generally divided into two stages (Deng 2008; Adapa *et al.* 2009). In the initial stage of crushing, lower pressure is transmitted to the biomass particles, causing the originally loosely packed solid particles to change their arrangement, reducing the internal void ratio of the biomass. When the pressure gradually increases, the large biomass particles break under the action of the pressure, become smaller particles, and undergo plastic flow or deformation. At this time, the particles begin to fill the gaps and come into closer contact, and part of the residual stress is stored inside the forming block, making the bonds between the particles stronger. In this process, the deformation of the biomass material structure can absorb a great amount of energy.

Paper scraps were employed as the filler of the thin-walled tube in this work. Such scraps not only can increase the specific energy absorption of the whole structure, but also they can exhibit many other characteristics. Paper scraps are flammable materials, but the density of paper scraps as filler is quite high, which leaves little room for oxygen among them. In addition, adding flame retardant to paper scraps can prevent combustion. Paper scraps are similar to aluminum foam, enhancing the crashworthiness properties through their occupation of space. When the paper scraps are compressed axially, the mean

crushing force is increased by squeezing the air inside. This behavior may be a way to further improve the energy absorption performance of paper scraps (Wang 2000; Ju 2012). The foamed structure has advantages of low density, high shock absorption capacity, sound insulation and noise reduction, low thermal conductivity, high electromagnetic shielding, easy processing, easy installation, and high forming accuracy (Chen *et al.* 2002; Lu *et al.* 2006).

This study attempted to replace the foamed aluminum with biomass material for thin-walled tube filling, to reduce the cost of materials while maintaining its excellent energy absorption characteristics. Quasi-static crushing tests and numerical simulations by using the explicit non-linear finite element software LS-DYNA were used to test the improvements of the mean crushing force and specific energy absorption characteristics of thin-walled tubes by filling them with different densities of paper scraps. Quasi-static crushing tests were performed for empty thin-walled tube, paper scraps, and thin-walled tube filled with paper scraps, and corresponding numerical simulation was carried out to compare with the test results.

### Crashworthiness Parameters

Crashworthy design of thin-walled structures requires a good energy absorption capacity, which is usually characterized by the following parameters: initial peak force (*IPF*), mean crushing force (*MCF*), absorbed energy (*EA*), crush force efficiency (*CFE*) and specific energy absorption (*SEA*).

Initial peak force (*IPF*) is the first peak force that appears in the load-displacement curve:

$$IPF = \max(P(\delta)) \quad (1)$$

where  $P(\delta)$  is the crushing force (N), and  $\delta$  is the crushing distance (m).

Energy absorption (*EA*) can be obtained by calculating the integral of the relationship curve between crushing force and crushing distance (Eq. 2),

$$EA = \int_0^{\delta_f} P(\delta)d\delta \quad (2)$$

where  $P(\delta)$  is the crushing force (N), and  $\delta_f$  is the total crushing distance (m).

$$MCF = \frac{1}{\delta_f} \int_0^{\delta_f} P(\delta)d\delta \quad (3)$$

In Eq. 3,  $\delta_f$  is the total crushing distance (m).

Crush force efficiency (*CFE*) is the percentage ratio between *MCF* and *IPF*,

$$CFE = \frac{MCF}{IPF} * 100\% \quad (4)$$

where *MCF* is mean crushing force (N), and *IPF* is initial peak force (N).

Specific energy absorption (*SEA*) is the energy absorption per unit mass, which is an important parameter to evaluate the energy absorption capacity of different materials, as defined by Eq. 5,

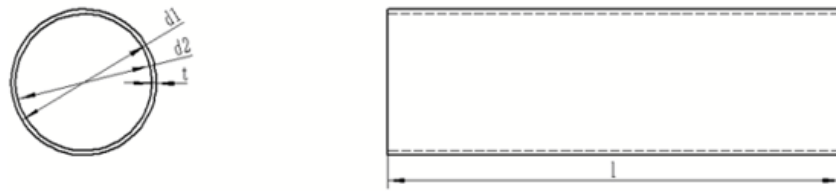
$$SEA = \frac{EA}{\rho Al_1} \quad (5)$$

where  $\rho$  is the density of the material ( $\text{kg/m}^3$ ),  $A$  is the tube cross sectional area ( $\text{m}^2$ ), and  $l_1$  is the length of the structure participating in the energy absorption (m).

## EXPERIMENTAL

### Materials

The material of thin-walled tube used in the tests was steel (Q345) of 0.6 mm thickness with the following mechanical properties from Table 1, and the geometry dimensions are shown in Fig. 1.



$$d_1 = 30.8\text{mm} \quad d_2 = 32\text{mm} \quad t = 0.6\text{mm} \quad l = 100\text{mm}$$

Fig. 1. Geometry and dimensions of the thin-walled tube

Table 1. Properties of Steel Q345

Properties	Value	Unit
Density	7800	$\text{kg/m}^3$
Elastic modulus	206	MPa
Poisson's ratio	0.28	-
Yield stress	375	MPa
Shear modulus	250	MPa

### Methods

The crushing tests were carried out using an electronic universal testing machine (RGM-2010, Shenzhen Reger Instrument Co., Ltd, Shenzhen, China) (Fig. 2). The maximum loading force was 10 kN, the test speed was 0.001 mm/min to 500 mm/min, and the sampling rate can reach 200 Hz.

The test was divided into three groups, namely the quasi-static crushing test of empty tube, paper scraps, and paper scraps filled tube. In the crushing test of empty tube, the bottom end of the empty tube was fixed on the platform, and axial crushing was performed from the top with the mechanical testing machine. The crushing stroke was 80 mm, and the loading speed of the crushing platen was 3 mm/min.

To determine the crushing characteristics of paper scraps, a quasi-static crushing test was carried out. First, use a homemade paper scraps crushing tool (Fig. 6) to press different qualities of scraps into the steel tube to form a cylinder with the same volume (100 mm in height and 30.8 mm in diameter) and a density of 0.2 to 0.6  $\text{g/cm}^3$ . Next, in order to prevent the paper scraps from collapsing and dispersing in the crushing process and ensure that the strain mainly occurs in the axial direction, the paper scraps cylinders with different densities were placed in the steel tube, and the paper scraps cylinder was

compressed to a height of 10 mm by using the mechanical testing machine and the paper scraps crushing tool.

In the test of the pipe filled with paper scraps, the steel tube was filled with paper scraps with the density of 0.2 to 0.6 g / mm<sup>3</sup>, and the whole structure was compressed quasi statically. The loading speed of the crushing platen was 3 mm/min.



**Fig. 2.** Electronic universal testing machine

### Numerical Model

The numerical models of empty steel tube and steel tube filled with different density paper scraps were established by using the finite element software LS-DYNA (Version 970; Livermore Software Technology Corporation, Livermore, CA, USA) to simulate their quasi-static crushing tests. The numerical model consists of two parts: the test piece (empty tube or paper filling tube) and the pressure plate of the mechanical testing machine (Fig. 3).

In LS-DYNA software, the material definition method is to fill in material cards, each type of material has its own material card number, and 26, 63, 75, and 126 materials model are all foam materials. After comparing the simulation results of these four materials, the 63 material model was selected for modeling. The material was specially used to model compressible foam. Its stress-strain curve is shown in Fig. 4 (Livermore Software Technology Corporation 2013).

This material follows the constitutive relationship of foam (Eq. 6),

$$\sigma_y = k\varepsilon^n = k(\varepsilon_{yp} + \bar{\varepsilon}^p)^n \quad (6)$$

where  $\sigma_y$  is the yield stress (Pa),  $\varepsilon_{yp}$  is the elastic strain to yield,  $\bar{\varepsilon}^p$  is the effective plastic strain (logarithmic),  $k$  is the strength coefficient (Pa),  $n$  is the hardening exponent, and  $p$  is the strain rate parameter.

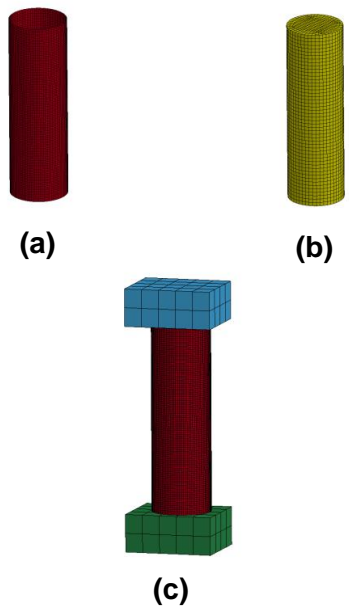


**Fig. 3.** The numerical model of each part: (a) Thin-walled steel tube; (b) paper scraps cylinder; (c) The whole model (specimens, top and bottom platens)

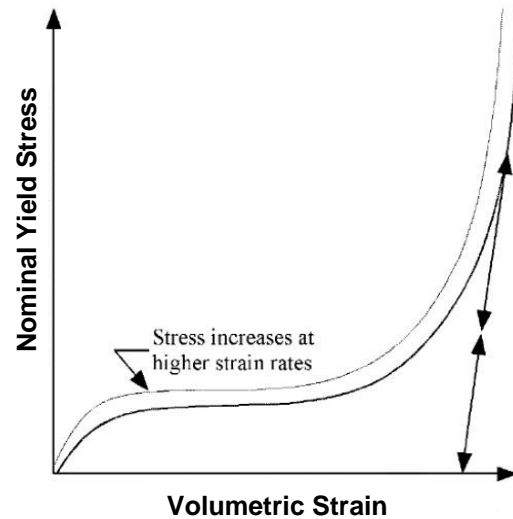


**Fig. 4.** Stress-strain curves of Crushable Foam #63

Based on the stress and strain data of the paper scraps obtained in the tests, the yield stages of paper scraps and foamed aluminum have certain commonalities. In addition, the test data of the 63 material model is consistent with the test data of foamed aluminum (Hanssen *et al.* 2000). Therefore, the 63 material model could be used to simulate the paper scraps.

The material of paper scraps was simulated by the 63 ‘MAT CRUSHABLE FOAM’ with mechanical properties of Elastic modulus ( $E = 200$  MPa) and Poisson’s ratio ( $\mu = 0.04$ ). The curve (Fig. 8) obtained from the tests was taken as the stress-strain curve of the material. The mesh of paper scraps consisted of 14416 solid elements (eight noded hexahedrons) (Fig. 3b).

The tube material was modelled with the material model 24 ‘MAT PIECE-WISE LINEAR PLASTICITY’, introducing the properties from Table 1. The models of tube were discretised using the computationally efficient four-node Belytschko-Tsay shell element (Hallquist 2006). To accurately describe the deformation, the element size was set to 1 mm, and a total of 6108 shell elements were obtained (Fig. 3a).

Material model 20 ‘MAT RIGID’ was assigned to the crushing platens of testing machine, which are practically not deformed during a crushing test. One eight-noded ‘brick’ element was used to model the lower and upper platens. The lower crushing platen of the testing machine was fixed, and the upper crushing platen can only move up and down axially. To reduce the simulation time under the condition of accurately simulating quasi-static crushing test, the speed of upper platen was set to be 1 m/s, which was higher than the test speed of 3 mm/min. At this speed, the kinetic energy of specimens was negligible compared with their internal energy (Wang and Fan 2003).

The Coulomb contact types ‘nodes to surface’ and ‘surface to surface’ were selected to respectively simulate the platen-tube interaction and the platen-paperscraps and tube-paperscraps interaction. The contact surfaces on the platens were specified as the

'master' surfaces, whereas the shell edge nodes and the contact surface on paper scraps were defined as the 'slave' nodes and the 'slave' surfaces respectively. 'Self contact' type was defined to simulate the situation during the collapse when elements of the tube wall or of the paper scraps outer surface contact each other. The static and dynamic coefficients were respectively set as 0.3 and 0.15 for the platen-tube, platen-paperscraps and tube-paperscraps interaction, and as 0.3 and 0.3 for the 'self contact' of tube wall and paper scraps outer surface.

After the reliability was verified (Section: Results and Discussion), The numerical simulation was used to study the performances of different structures, and the paper scraps structure with the best performance was identified. Optimizing the filler's structure is a common approach to increase specific energy absorption, and the main methods include changing the shape of the filler structure and adopting a multilayer or polygonal structure (Marzbanrad and Ebrahimi 2011; Shi *et al.* 2013; Sun *et al.* 2017). Meanwhile, combined with the test results of filled steel tube, the following three paper scraps filling structures were designed: a cross structure, a double-layer structure, and cross double-layer structure, as shown in Fig. 5. The geometric dimensions and densities of three structures are shown in Table 2.

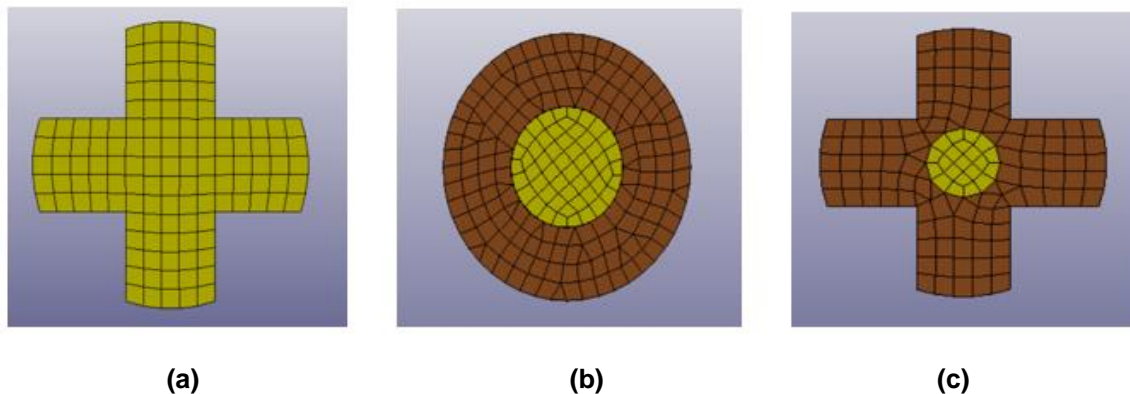


**Fig. 5.** Three kinds of paper scraps filling structures: (a) Cross structure; (b) Double-layer structure; (c) Cross double-layer structure

**Table 2.** Geometric Dimensions and Densities of the Three Structures

Structure	Inner Layer Diameter (mm)	Outer Layer Diameter (mm)	Inner Layer Density (g/cm <sup>3</sup> )	Outer Layer Density (g/cm <sup>3</sup> )
Cross	0	30.8	0	0.2
Double-layer	12	30.8	0.6	0.2
Cross double-layer	8	30.8	0.6	0.2

## RESULTS AND DISCUSSION

### Experimental and simulation results

The test and simulation results of the empty thin-walled tube after quasi-static crushing are shown in Fig. 6(a) and 6(b), and the load displacement curve of empty tube during crushing is shown in Fig. 7.



**Fig. 6.** Empty thin-walled tube after crushing test and simulation: (a) Test result; (b) Simulation result

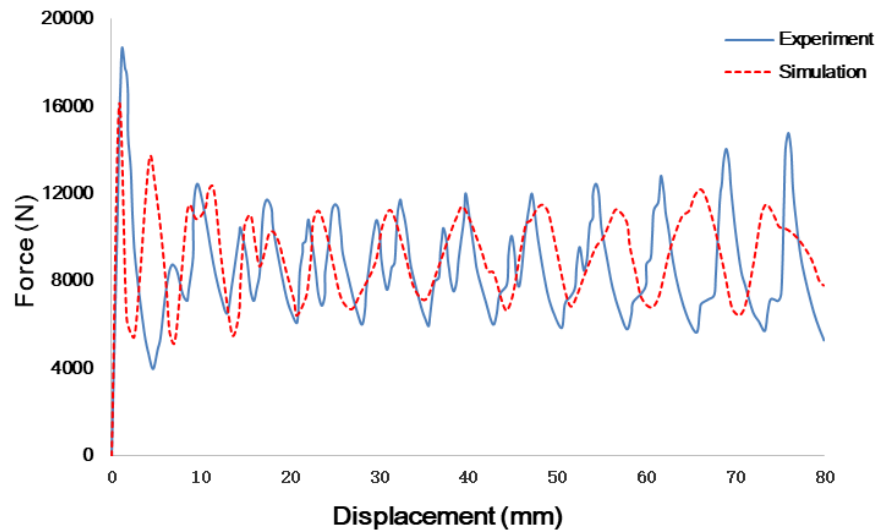


**Fig. 7.** Comparison between simulation and test of empty thin-walled tube

**Table 3.** Mean Crushing Force (MCF) and Specific Energy Absorption (SEA) of Empty Tube

Group	MCF (kN)	Simulation error (%)	SEA (kJ/kg)	Simulation error (%)
Test group	8.64	-	18.5	-
Simulation group	8.23	4.74	17.6	4.8

Table 3 shows the simulation and test values of the mean crushing force (MCF) and specific energy absorption (SEA) of the empty tube subjected to quasi-static axial crushing.

As shown by Fig. 6, Fig. 7, and Table 3, the simulation results of the quasi-static axial crushing of the empty tube were in good agreement with the test results. The mean crushing force and specific energy absorption of the test group were slightly higher than those of the simulation group, with the error being 4.8%. This discrepancy is because the tube itself may have local defects, and the material distribution may be uneven. Therefore, there were some differences between the results of the simulation and the test, but the errors were still within the acceptable range (Generally, it is acceptable that the error between the

numerical simulation and test results is less than 5%).

Figure 8 shows the load-displacement curve during quasi-static crushing of paper scraps. The test results showed that the stress-strain curves of paper scraps crushing could be divided into two stages: the stage of yield platform and the stage of densification.

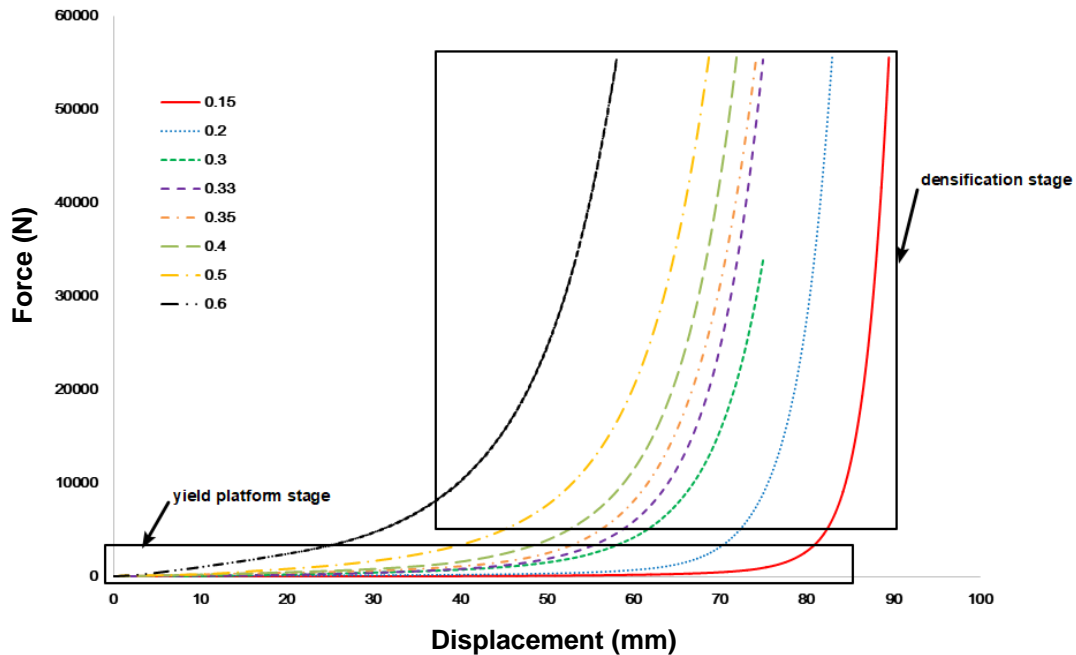


Fig. 8. Load-displacement curves of paper scraps

Figures 9(a) and 9(b) are the compressed tube filled with paper scraps and its half section respectively, and the load-displacement curve of the tube during the crushing process is shown in Fig. 10.

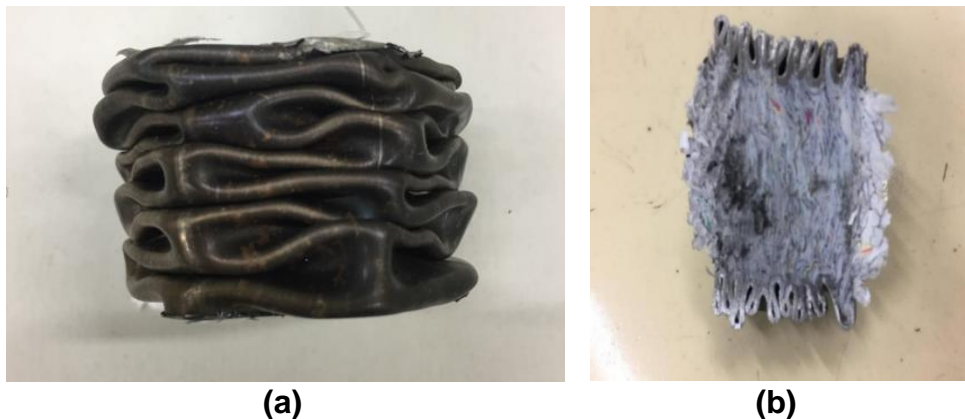


Fig. 9. Thin-walled tube filled with paper scraps after crushing test: (a) The whole tube; (b) Half section of tube

When the strain was small, the paper scraps yielded after compression, and the yield platform appeared. At this time, with the increase of strain, the stress increased slowly, which mainly reflected the collapsing and yielding of the gap structure of the paper scraps. Lower pressure was transferred to the particles of the paper chips, changing the arrangement of the previously loosely packed solid particles and leading to the decrease of

the internal void ratio of the paper scraps.

As the paper scraps were compacted, the stress increased rapidly and entered the densification stage. Large biomass particles broke under great pressure and became smaller particles, which deformed or flowed plastically. At this point, the particles began to fill the voids and engage with each other more closely. Some of the residual stress was stored within the structure, making the bonding between particles stronger. This stage reflected the deformation of the paper scraps after compaction.

As shown from the crushing deformation mode of the paper scraps, the paper scraps structure was very similar to that of aluminum foam, but its platform stage was not obvious, and the whole curve basically showed an exponential growth process. Furthermore, the appearance of its densification is related to the density of the paper scraps themselves. With greater density, densification appeared earlier.

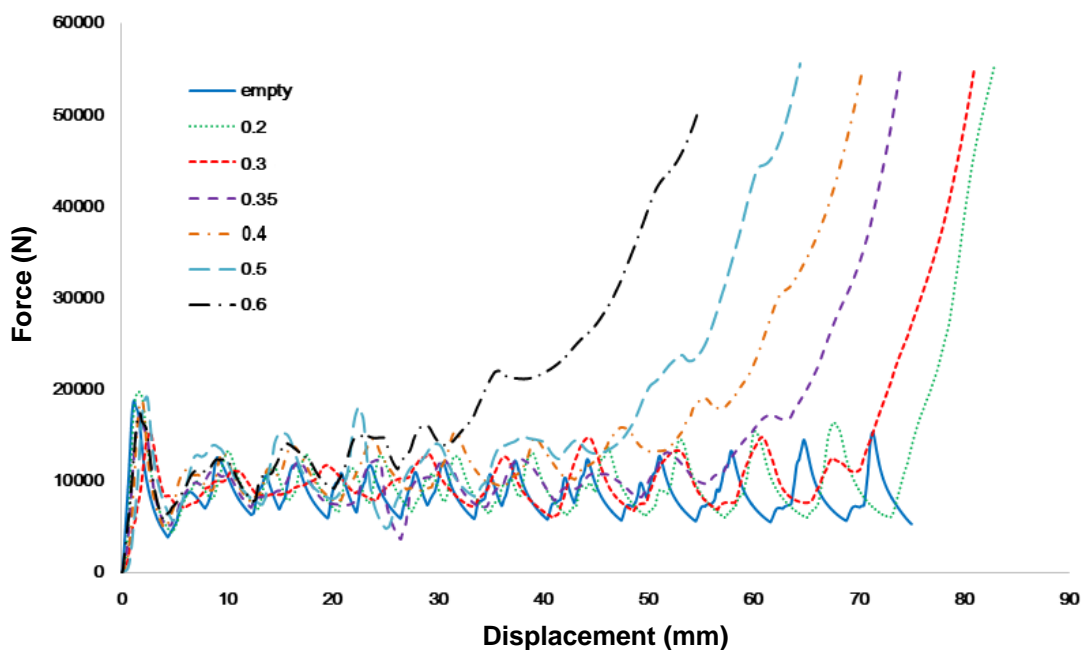


**Fig. 10.** Load-displacement curves of thin-walled tubes filled with different densities of paper scraps

In the whole deformation process, the thin-walled tube played a leading role at the beginning. Thus, the curve had a rapid decrease after the sharp increase, which was in line with the pressure change during the collapse of the empty tube. After that, the curve fluctuated with a single increasing curve due to the rapid increase of the crushing force in the densification stage. Finally, the paper scraps pressure rose to the leading role, and the curve increased exponentially, reaching the critical point quickly.

The simulation results are shown in Fig. 11. Four segments of the tube crushing are shown in this figure. As the crushing displacement of the crushing platen increased, the strain of the tube and the paper scraps increased and advanced with the folding of the tube. From the deformation pattern of the filler, compared with the empty thin-walled tube, the half-wavelength of fold buckling increased when the thin-walled tube filled with paper scraps deformed under crushing.

As shown from Table 4 and Fig. 12, the specific energy absorption of the steel tube was increased to a certain extent by filling with paper scraps. When the paper scraps density

was in the range 0.2 to 0.6 g/cm<sup>3</sup>, the specific energy absorption performance of paper scraps filling tube was improved compared with the empty tube. Among them, the filling tube with a paper scraps density of 0.6 g/cm<sup>3</sup> yielded the largest increase in specific energy absorption, which was 9.7%, followed by 9.4% of 0.35 g/cm<sup>3</sup> paper scraps. In addition, the mean crushing force of the steel tube filled with paper scraps was also greatly improved. Therefore, paper scraps were a good material for energy absorbing.

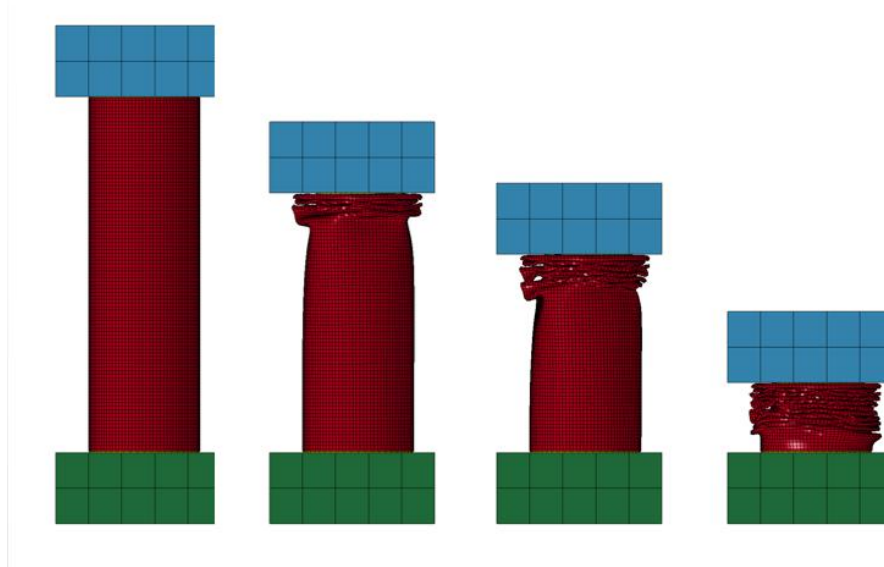
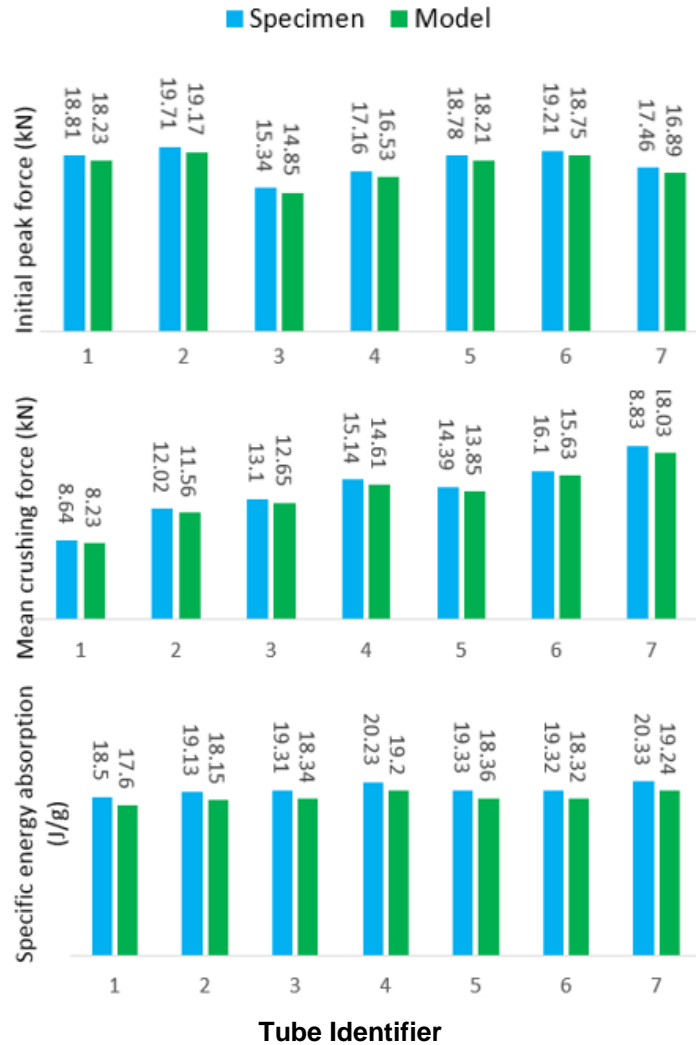


Fig. 11. Crushing process of thin-walled tube filled with paper scraps

Table 4. Crashworthiness Parameters of the Specimens (Experimental and simulation results)

Identifier	Tube type	Paper scraps density (g/cm <sup>3</sup> )	Mass (g)	IPF (kN)	EA (J)	MCF (kN)	Improvement of MCF Compared with Empty Tube (%)	SEA (J/g)	Improvement of SEA Compared with Empty Tube (%)	CFE (%)
1	Specimen	-	46.2	18.81	691.2	8.64	-	18.5	-	45.93
	Model			18.23	658.4	8.23	-	17.6	-	45.15
2	Specimen	0.2	61.1	19.71	961.6	12.02	39.1	19.13	3.4	60.98
	Model			19.17	924.8	11.56	40.46	18.15	3.1	60.30
3	Specimen	0.3	68.6	15.34	1048.0	13.10	51.5	19.31	4.4	85.40
	Model			14.85	1012.0	12.65	53.71	18.34	4.2	85.19
4	Specimen	0.35	72.3	17.16	1211.2	15.14	75.6	20.23	9.4	88.23
	Model			16.53	1168.8	14.61	77.52	19.20	9.1	88.38
5	Specimen	0.4	76.0	18.78	1151.2	14.39	66.9	19.33	4.7	76.62
	Model			18.21	1108.0	13.85	68.29	18.36	4.3	76.06
6	Specimen	0.5	83.5	19.21	1288.0	16.10	86.3	19.32	4.5	83.81
	Model			18.75	1250.4	15.63	89.91	18.32	4.1	83.36
7	Specimen	0.6	90.9	17.46	1506.4	18.83	117.4	20.33	9.7	107.85
	Model			16.89	1442.4	18.03	119.08	19.24	9.3	106.75



**Fig. 12.** Comparative charts for the initial peak force, mean crushing force and specific energy absorption between the specimens and the numerical models

### Interaction between Paper Scraps and Steel Tube

When foamed aluminum is used as a filler, the main pressure increase comes from the interaction between the foamed aluminum and the thin-walled tube. The interaction of foam aluminum is generally attributed to the following two reasons (Hanssen *et al.* 2000; Wang *et al.* 2007): First, there is greater external and inward folding resistance in the presence of foam filler in thin-walled components, so the wavelength of plastic folding decreases, and the number of folds increases during progressive axial collapse. Second, the interfacial friction stress within the filler and the interaction between the material and the tube wall makes the pressure of the tube filled with aluminum foam higher than the total pressure of the empty tube and aluminum foam when compressed separately. Therefore, the mean crushing force of the filled tube can be divided into three parts: (1) the average force of the empty tube, (2) uniaxial resistance of the filler, and (3) the interaction force between the empty tube and the filler. Similar interaction can also be found in the crushing tests of the tubes filled with paper scraps.

Eq. 7 defines the interaction force ( $P_i$ ):

$$P_i = P_{c,f} - P_c - P_f \quad (7)$$

where  $P_{c,f}$  is the mean crushing force of filled tube,  $P_c$  is the average force of empty tube, and  $P_f$  is the average force of paper scraps.

With the previous test data, the interaction forces between the paper scraps with different densities and the tube under axial crushing were calculated (Table 5 and Fig. 13).

As shown in Table 5 and Fig. 13, the interaction force played an important role in the crushing of the tube filled with paper scraps. When the density of the paper scraps was  $0.35 \text{ g/cm}^3$ , the interaction force was the largest, and the ratio between the interaction force and the force of the paper scraps was also the largest. As shown, the increase of the mean crushing force of the tube filled at a density of  $0.6 \text{ g/cm}^3$  was mainly due to the average force of the paper scraps ( $P_f$ ). The crushing strength of the  $0.35 \text{ g/cm}^3$  paper scraps mainly depended on the interaction.

**Table 5.** Interaction Forces with Different Densities of Paper Scraps

Density of Paper Scraps ( $\text{g/cm}^3$ )	Interaction Force ( $P_i$ ) (kN)	Average Force of Paper Scraps ( $P_f$ ) (kN)	$P_i / P_f$
0.2	1.548	1.832	0.84
0.3	1.861	2.599	0.72
0.35	3.178	3.322	0.96
0.4	2.086	3.664	0.57
0.5	2.687	4.773	0.56
0.6	2.355	7.835	0.30

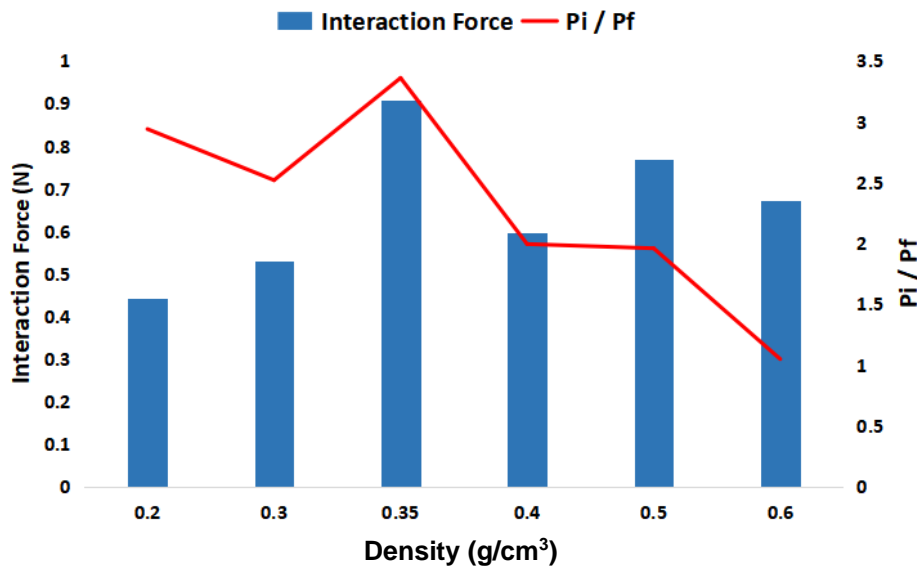


**Fig. 13.** Interaction forces between paper scraps with different densities and the tube

### Optimization of Paper Scraps Filling Structure

Using the numerical method to simulate crushing process of new structures of paper scraps filling, the deformations and load-displacement curves of three structures were obtained (Figs. 14 and 15). As shown in Fig. 14, the folds of cross double-layer structure were the largest and the fewest, allowing more paper scraps to enter and enhancing the interaction. This viewpoint can be verified by calculating the specific energy absorption of

structures. As shown in Fig. 15, the increase in the mean crushing force of cross structure was slower than that of the double-layer structure because it reduced the volume of the paper scraps by approximately one third. Compared with the cross structure, the cross double-layer structure had a certain improvement on the crushing force without increasing mass. The specific energy absorption and specific energy absorption improvements of the three structures were calculated, as shown in Table 5.

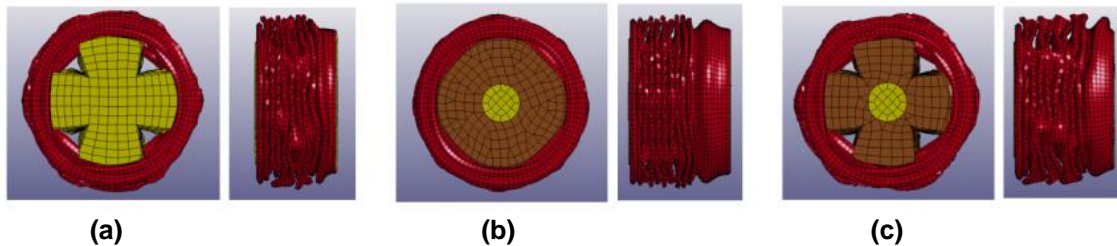


**Fig. 14.** Deformations of three structures: (a) Cross structure; (b) Double-layer structure; (c) Cross double-layer structure

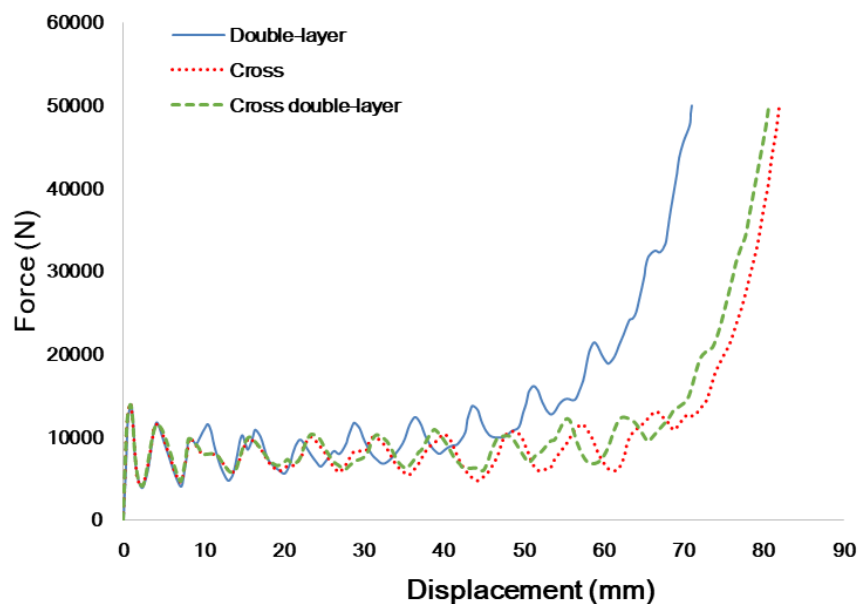


**Fig. 15.** Load-displacement curves of three structures

**Table 6.** Specific Energy Absorption and Improvements of Three Structures

Structure	SEA (J/g)	Improvement of SEA Compared with Empty Tube (%)
Cross	19.77	6.86
Double-layer	19.92	7.68
Cross double-layer	20.28	9.62

The cross double-layer structure exhibited the best improvement of specific energy absorption. Therefore, based on this structure, the energy absorption characteristics of the structure were further improved by changing the diameter and the density of the inner layer

without changing the total mass of the inner layer. Using finite element simulation tests of the cross double-layer structure with different densities and diameters of the inner layer, the optimal inner layer density under each diameter was found, and the specific energy absorption enhancement was calculated.

The general relationship between the specific energy absorption of the structure with optimal density and the diameter of its inner layer was fitted, and the curve is shown in Eq. 8 and Fig. 16:

$$SEA = -0.0046 d^3 + 0.05 d^2 - 0.039 d + 19.95 \quad (8)$$

where  $d$  (mm) is the inner-layer diameter.

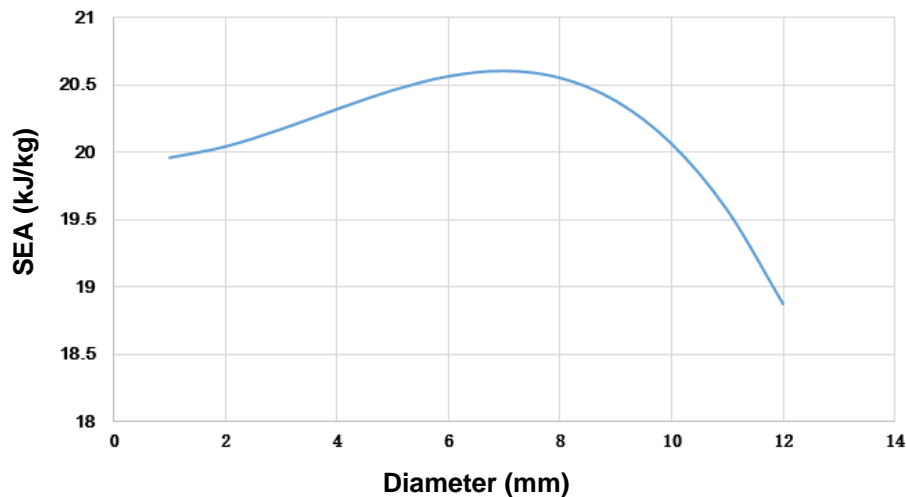


Fig. 16. SEA curve of optimal density of inner layer of cross double-layer structure

It was found from the curve that the optimal diameter and density of the inner layer of the cross double-layer structure were 6.98 mm and 0.79 g/cm<sup>3</sup>, at which point the specific energy absorption was 20.60 kJ/kg, and the SEA was increased by 11.35%, and the total mass of the structure was reduced effectively.

## CONCLUSIONS

In this study, the axial crushing of thin-walled steel tubes was investigated both experimentally and numerically by employing the explicit non-linear finite element software LS-DYNA. Quasi-static axial crushing tests were carried out on empty tube, paper scraps and tube filled with paper scraps respectively, and corresponding numerical models were established to simulate crushing tests. Finally, after verifying the accuracy of numerical models, the numerical method was used to find a better paper scraps filling structure. The main conclusions were as follows:

1. The quasi-static crushing tests and numerical simulation results showed that the density of the paper scraps had a certain influence on the energy absorption capacity of the tube filled with paper scraps. When the density of the paper scraps was 0.35 g/cm<sup>3</sup>, the specific energy absorption increased by 9.4%.
2. According to the formula of the interaction relationship, it was found that the increase

of collapse force of the filled tube was mainly due to the interaction between paper scraps and the steel tube, reaching a maximum when the density of paper scraps was  $0.35 \text{ g/cm}^3$ .

3. The cross double-layer paper scraps filling structure obtained by structure optimization improved the specific energy absorption up to 11.35% with an inner-layer diameter of 6.98 mm and density of  $0.79 \text{ g/cm}^3$ .
4. Due to its characteristics of low cost, simple preparation, and near-zero pollution, paper scraps have the potential to be used as a new material in thin-walled tube fittings of vehicles to increase vehicle crash safety.

## ACKNOWLEDGMENTS

The authors are particularly grateful for the test equipment support of Mr. Zhang Jianzhong and Mr. Chen Zhongjia, which enabled the successfully completion of the compression tests in this study.

## REFERENCES CITED

- Adapa, P. K., Tabil, L. G., and Schoenau, G. J. (2009). "Compression characteristics of selected ground agricultural biomass," *Agricultural Engineering International: The CIGR Ejournal* 11(6), manuscript 1347.
- Ali, M., Miller, J., Kim, S., Takak, S., and Kara, T. (2010). "A finite element study of a foam filled composite graded cellular structure," in: *Proceedings of the 2010 IEEE 36th Annual Northeast Bioengineering Conference (NEBEC)*, New York, NY, USA, pp. 1-2. DOI: 10.1109/nebc.2010.5458259
- Baroutaji, A., Sajjia, M., and Olabi, A.-G. (2017). "On the crashworthiness performance of thin-walled energy absorbers: Recent advances and future developments," *Thin-walled Structures* 118, 137-163. DOI: 10.1016/j.tws.2017.05.018
- Chen, W., and Wierzbicki, T. (2001). "Relative merits of single-cell, multi-cell and foam-filled thin-walled structures in energy absorption," *Thin-walled Structures* 39(4), 287-306. DOI: 10.1016/S0263-8231(01)00006-4
- Chen, X., Zhao, W., Ma, Y., and Hu, A. (2002). "Present state, research and applications of foam metals development," *Powder Metallurgy Technology* 2002(03), 50-55. Code: CNKI:SUN:HBGB.0.2001-03-013
- Deng, B. (2008). *Biomass Briquetting's Characteristics and Finite Element Analysis*, Master's Thesis, Shandong University, Jinan, China.
- Goel, M. D. (2015). "Deformation, energy absorption and crushing behavior of single-, double- and multi-wall foam filled square and circular tubes," *Thin-walled Structures* 90, 1-11. DOI: 10.1016/j.tws.2015.01.004
- Gao, M., and Xu, P. (2016). "Pressing-crack energy absorption for aluminum foam filled aluminum shell under high value impact," *Ordinance Material Science and Engineering* 39(1), 45-49. DOI: 10.14024/j.cnki.1004-244x.20151215.001
- Hallquist, J. O. (2006). *LS-DYNA® Theoretical Manual*, Livermore, California, USA.
- Hanssen, A. G., Langseth, M., and Hopperstad, O. S. (1999). "Static crushing of square aluminium extrusions with aluminium foam filler," *International Journal of*

- Mechanical Sciences* 41(8), 967-993. DOI: 10.1016/S0020-7403(98)00064-2
- Hanssen, A. G., Langseth, M., and Hopperstad, O. S. (2000). "Static and dynamic crushing of circular aluminium extrusions with aluminium foam filler," *International Journal of Impact Engineering* 24(5), 475-507. DOI: 10.1016/S0734-743X(99)00170-0
- Jing, P., Chi, Y., Wang, J., Wang, H., Wang, Q., Yang, K., Kang, X., and Li, Y. (2012). "Manufacturing technology and application status of foamed metal," *Hot Working Technology* 41(22), 59-62. DOI:10.14158/j.cnki.1001-3814.2012.22.012
- Ju, Y. (2012). *Research on Environmental Protection Fiber Foaming Buffer Material*, Master's Thesis, Jiangnan University, Wuxi, China.
- Livermore Software Technology Corporation (2013). *LS—DYNA® Keyword User's Manual*, Vol. 2, Livermore, California, USA.
- Lu, T., He, D., Chen, C., Zhao, C., Fang, D., and Wang, X. (2006). "Multifunctional properties and applications of ultra light porous metal materials," *Advances in Mechanics* 2006(04), 517-535. Code: 5ae9c3f7c095d713d8968239
- Marzbanrad, J., and Ebrahimi, M. R. (2011). "Multi-objective optimization of aluminum hollow tubes for vehicle crash energy absorption using a genetic algorithm and neural networks," *Thin-walled Structures* 49(12), 1605-1615. DOI: 10.1016/j.tws.2011.08.009
- Shi, L., Zhu, P., Yang, R.-J., and Lin, S.-P. (2013). "Adaptive sampling-based RBDO method for vehicle crashworthiness design using Bayesian metric and stochastic sensitivity analysis with independent random variables," *International Journal of Crashworthiness* 18(4), 331-342. DOI: 10.1080/13588265.2013.793262
- Sun, G., Pang, T., Fang, J., Li, G., and Li, Q. (2017). "Parameterization of criss-cross configurations for multiobjective crashworthiness optimization," *International Journal of Mechanical Sciences* 124-125, 145-157. DOI: 10.1016/j.ijmecsci.2017.02.027
- Tang, X. (2018). *Study on Axial Compression of Foam-filled CFRP Thin-walled Tubes*, Master's Thesis, Dalian University of Technology, Dalian, China.
- Wang, M. (2000). "The property and prospect of the corrugated paper board," *Packaging Engineering* 21(004), 5-8. DOI: 10.3969/j.issn.1001-3563.2000.04.003
- Wang, Q., and Fan, Z. (2003). "Improvement in analysis of quasi-static collapse with LS-DYNA," *Mechanics in Engineering* 2003(3), 20-23. DOI:10.6052/1000-0992-2001-498
- Wang, Q., Fan, Z., Song, H., Gui, L., Wang, Z., and Fu, Z. (2004). "Experimental studies on the axial crushing behaviors of aluminum foam-filled hat sections," *Chinese Journal of Mechanical Engineering* 40(11), 98-102. DOI: 10.3321/j.issn:0577-6686.2004.11.018
- Wang, Q., Fan, Z., Gui, L., Wang, Z., and Fu, Z. (2005). "Energy absorption behavior of aluminium foam under medium strain rate," *Chinese Journal of Materials Research* 19(6), 601-607. DOI: 10.3321/j.issn:1005-3093.2005.06.007
- Wang, Q., Fan, Z., and Gui, L. (2007). "Theoretical analysis for axial crushing behaviour of aluminium foam-filled hat sections," *International Journal of Mechanical Sciences* 49(4), 515-521. DOI: 10.1016/j.ijmecsci.2006.06.011
- Wang, G. (2016). *Loading Path Based Aluminum Body Optimized Design of Electric Vehicle under Frontal Crashing*, Doctor's Thesis, Hunan University, Changsha, China.
- Xiong, F. (2018). *Research on Lightweight and Crashworthiness Multi-objective*

*Collaborative Optimization Design Method for Automobile Body Structure*, Doctor's Thesis, Jilin University, Changchun, China.

Yang, X., Xu, J., Zou, T., Zhao, N., and Zong, R. (2019). "Advances in the composite structure of aluminum foam filled metal thin-walled tube," *Materials Reports* 33(21), 111-117. Code: CNKI:SUN:CLDB.0.2019-21-015

Ying, W., Wang, Y., and Zhai, X. (2018). "Experimental study of aluminum foam filled energy absorption connectors under impact loading," *Journal of Harbin Institute of Technology* 50(12), 171-177. DOI: 10.11918/j.issn.0367-6234.201802056

Zhang, H., and Ou Yang, B. (2020). "The performance characteristics of 'foam aluminum' and its application in automobile industry," *Powder Metallurgy Industry* 30(3), 79-82. DOI: 10.13228/j.boyuan.issn1006-6543.20190175

Article submitted: January 23, 2021; Peer review completed: February 28, 2021; Revised version received and accepted: July 10, 2021; Published: July 13, 2021.

DOI: 10.15376/biores.16.3.5985-6002